JOURNAL OF CATALYSIS **161,** 551–559 (1996)
ARTICLE NO. 0217

An X-Ray Photoelectron Spectroscopy Study of the Acidity of SiO_2–ZrO_2 Mixed Oxides

H. J. M. Bosman,[1] A. P. Pijpers, and A. W. M. A. Jaspers

Industrial Catalysis Section, DSM Research B.V., P.O. Box 18, 6160 MD Geleen, The Netherlands

Received March 7, 1995; revised February 26, 1996; accepted March 22, 1996

X-ray photoelectron spectroscopy (XPS) measurements on SiO_2–ZrO_2 mixed oxides with varying Si/Zr ratios are presented. The measurements yield interesting insight into surface properties which may help the understanding of their catalytic action. Especially, the surface acid properties of the catalysts are better understood. On the one hand, on SiO_2–ZrO_2 mixed oxides with 75 wt% or less ZrO_2, an increase of the positive charge on the Zr cation is observed compared to the single oxide ZrO_2. This is concluded from higher Zr3$d_{5/2}$ binding energies. The higher binding energy (charge) is indicative of strong Lewis acidity in the mixed oxides. On the other hand, oxygen associated with the Si cation in these mixed oxides appears to have a slightly higher electron density (base strength) than in the single-oxide SiO_2, as is concluded from the lower O1*s* binding energies (of oxygen near Si). This fact is an indicator for a small increase in the number of Brønsted acid sites. Furthermore, XPS shows that the surface of the mixed oxides containing 75 wt% or less ZrO_2 is depleted in zirconium. The surface Zr concentration determined with XPS is roughly 50% of the bulk value. This depletion is most probably due to differences in reactivity of the Si and the Zr precursors in the precipitation step and not due to phase separation in the calcination step. A noncalcined catalyst also shows surface depletion in Zr.

INTRODUCTION

It is known that SiO_2–ZrO_2 mixed oxides have extreme acid properties, whereas the single oxides show only a weak acidity (1–5). Both the type of acid sites (Lewis/Brønsted) and their strength will influence the catalytic activity. X-ray photoelectron spectroscopy (XPS) studies have the potential to yield detailed information on the type of the acid sites, as well as information on surface concentrations.

XPS is not used very often as a technique for the characterization of the acidity of catalysts. However, a few research groups have studied SiO_2–Al_2O_3 catalysts (especially zeolites) by XPS. Wagner *et al.* (6), Barr and Lishka (7, 8), Okamoto *et al.* (9), and Casamassima *et al.* (10, 11) give detailed information on binding energies from characteristic Si, Al, and O lines. They derive interesting information on the nature of cation–oxygen bonds in the mixed oxides compared to the single oxides. This helps to understand the origin of the acidity of the catalysts under study. Only one article dealing with XPS on SiO_2–ZrO_2 is known to us, namely that of Slinkin *et al.* (12). In this paper the authors describe the influence on the texture and structure of SiO_2 brought about by chemical mixing with Al^{3+}, Ti^{4+}, and Zr^{4+} cations. Here also the XPS data yield information on the nature of the cation–oxygen bonds present in the mixed oxides, enabling conclusions to be drawn on their acidity.

EXPERIMENTAL

Preparation of Catalysts

Two series of SiO_2–ZrO_2 catalysts have been prepared via basic hydrolysis of mixtures of H_2SiF_6 and H_2ZrF_6 using ammonia at a constant pH of 9.0. The resulting precipitate was subsequently filtered, washed several times with distilled water, dried at 373 K, and calcined at 823 K. The catalysts are coded Si_xZr_y in which x and y give the respective amounts of SiO_2 and ZrO_2 in weight percent. The complete preparation procedure is described in detail elsewhere (1).

The two series differ in the amount of residual fluorine on the catalyst surface, as will follow from the XPS measurements described here. The first series (denoted A) was studied extensively and characterized earlier (BET specific surface area and pore volume, NH_3 TPD, XRD, IR, test reaction) (1, 2). The second series (denoted B) has been used for the first time in this investigation and was prepared to yield a more detailed insight into the properties of the mixed oxides. The difference in residual fluorine concentration is not completely understood, but is probably due to small differences in the precipitation procedure. We will discuss this feature in more detail later.

BET Specific Surface Area

Total (BET) specific surface areas were determined from physical adsorption of N_2 at $T = 78$ K, by applying the BET equation on the part of the adsorption isotherm with $0.05 \leq p/p_0 \leq 0.35$, measured in a Micromeritics Digisorb 2600 apparatus.

---

[1] To whom correspondence should be addressed. Fax: +31 46 4761298.

0021-9517/96 $18.00

X-Ray Diffraction Measurements

The single and mixed oxides were studied by X-ray diffraction, employing a Philips PW 1730 diffractometer equipped with a Cu anode and a nickel filter. The diffractograms were recorded using the Cu$K\alpha$ line (wavelength = 1.5418 Å) at $3^\circ < 2\theta < 60^\circ$.

X-Ray Photoelectron Spectroscopy Measurements

Samples were mounted with the aid of double-sided sticky tape on a sample holder and inserted via a separately pumped load lock into the Leybold MAX200 XPS instrument for measurement. No special care was taken after calcination of the samples and during transfer to the XPS instrument to prevent adsorption of moisture. Mg$K\alpha$ (1253.6 eV) radiation from a Mg/Al twin-anode X-ray source (13 kV, 20 mA) was used. The spectrometer has been calibrated using Ag, Cu, and Au (13). Using a pass energy of 48 eV the full width at half maximum (FWHM) for the Ag3$d_{5/2}$ line was 1.0 eV. The base pressure in the analysis chamber was well below 1×10^{-9} mbar (1×10^{-7} Pa) during the measurement. The instrument was controlled by a HP A400 computer, and a Leybold DS100 data system was used for data acquisition and analysis. For the quantitative analysis the spectra were corrected for the analyzer transmission function according to Ref. (14), and sensitivity factors were calculated according to the approach of Nöller *et al.* (15) and using the Scofield cross-sections (16). For energy referencing, a number of approaches are discussed by Briggs and Seah (17). Mullins and Averbach (18) and Stephenson and Binkowski (19) proposed bias-referencing techniques. The adventitious carbon contamination on the powder samples was chosen for energy referencing: the C1*s* binding energy at 284.6 eV was used.

RESULTS

Summary of Results Obtained in Earlier Work

The SiO_2–ZrO_2 catalysts have been studied by a number of techniques already, such as measurement of BET specific surface area and pore volume, NH_3 TPD, XRD, IR, and the dehydration of cyclohexanol as a test reaction (1, 2) which yielded preliminary insight into the catalytic and other properties. Chemically mixing SiO_2 and ZrO_2 yields materials with strong acid sites ($-13.8 < H_0 < -11.4$), whereas the single oxides are only weakly acidic (SiO_2: $+2.8 < H_0 < +4.0$; ZrO_2: $+0.8 < H_0 < +2.8$) (1). DRIFTS measurements of ammonia-treated or pyridine-treated samples show the strong acid sites to be of the Lewis type (2). However, Brønsted sites of weaker acidity are also found to be present.

Specific Surface Areas

Table 1 gives the BET specific surface areas measured. It can be seen that the surface area drops as the ZrO_2 content in the mixed oxides increases, but it is not a smooth decrease as a function of Zr content. However, the specific surface areas of the catalysts of series A and B of a certain composition are of the same order of magnitude, so residual fluorine does not have a large influence on this parameter.

TABLE 1

BET Specific Surface Areas of SiO_2–ZrO_2 Catalysts Examined in this Study

Series	Catalyst	BET specific surface area (m^2/g)
A	$Si_{100}Zr_0$	105
	$Si_{99}Zr_1$	n.d.
	$Si_{87}Zr_{13}$	117
	$Si_{75}Zr_{25}$	131
	$Si_{50}Zr_{50}$	42
	$Si_{25}Zr_{75}$	108
	Si_0Zr_{100}	12
B	$Si_{100}Zr_0$	113
	$Si_{95}Zr_5$	117
	$Si_{90}Zr_{10}$	51
	$Si_{75}Zr_{25}$	87
	$Si_{50}Zr_{50}$	36
	$Si_{25}Zr_{75}$	17
	$Si_{18}Zr_{82}$	n.d.
	$Si_{10}Zr_{90}$	32
	Si_5Zr_{95}	24
	Si_0Zr_{100}	21

Note. n.d., not determined.

X-Ray Diffraction

XRD measurements show that catalysts containing 82 wt% or more ZrO_2 are crystalline and have the baddeleyite structure. Apparently, the presence of small amounts of SiO_2 in ZrO_2 (bulk ratio $Si/Zr \leq 0.31$ (w/w)) does not alter the catalyst structure to a significant extent. Catalysts containing 75 wt% ZrO_2 or less are X-ray amorphous, as was reported previously (1).

X-Ray Photoelectron Spectroscopy

Figure 1 gives an example of an overall XPS spectrum of a Si-rich mixed oxide ($Si_{75}Zr_{25}$ B) together with peak assignments. Table 2 gives the surface composition of the catalysts as analyzed by XPS. XPS analyzes the outer 2 to 10 atom layers of a specimen (20, 21); the composition given is thus an average over the analysis depth. Values given in Table 2 exclude carbon and nitrogen. The total amount of C varies between 3 and 45 at% on the surface. Nitrogen is only present on noncalcined catalysts. For a correct quantitative analysis the relative intensity of energy loss lines must be taken into account, since the intensity of the O1*s* energy loss line is significantly higher than that of the other XPS lines (see Fig. 1). Hence, using only the main line intensities in the quantitative analysis of these mixed oxides

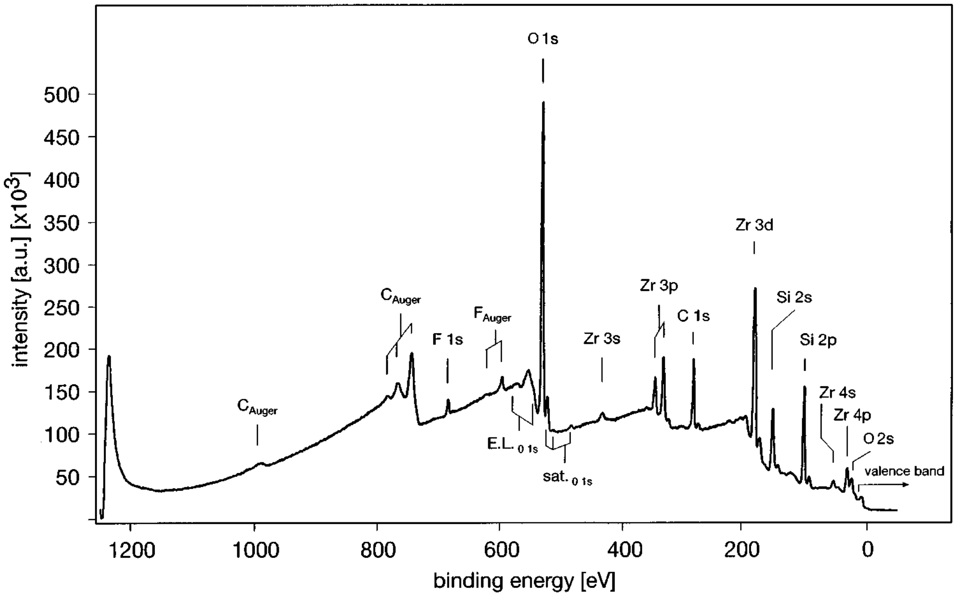

FIG. 1. Wide-scan XPS spectrum of the $Si_{75}Zr_{25}$ catalyst of series B.

would suggest too low an oxygen concentration. This behavior was already discussed in Ref. (18). For that reason the oxygen concentrations reported for series A in a previous paper (1) show too low a value. Table 3 gives the binding energies of several characteristic lines observed. It appears that significant changes can be observed in the spectra as a function of the ZrO_2 content of the mixed oxides, as will be discussed in detail below.

TABLE 2

Surface Concentrations of Zr, Si, O, and F (Leaving Out C and N) of the Various SiO_2–ZrO_2 Catalysts Calcined at 773 K Using XPS (Relative Accuracy 10%)

		Concentration (atom%)			
Series	Catalyst	Zr	Si	O	F
A	$Si_{100}Zr_0$	0.0	33.4	66.1	0.5
	$Si_{99}Zr_1$	0.1	32.8	66.5	0.7
	$Si_{87}Zr_{13}$	1.3	31.6	66.4	0.8
	$Si_{75}Zr_{25}$	2.9	29.4	67.0	0.6
	$Si_{50}Zr_{50}$	7.2	25.5	66.5	0.8
	$Si_{25}Zr_{75}$	6.1	25.5	67.5	0.8
	Si_0Zr_{100}	33.2	0.8[a]	63.9	2.1
	$Si_{25}Zr_{75}$ u	3.1	28.4	65.7	2.8
B	$Si_{100}Zr_0$	0.0	33.4	64.9	1.7
	$Si_{95}Zr_5$	0.5	32.2	65.5	1.9
	$Si_{90}Zr_{10}$	1.2	31.4	65.5	1.9
	$Si_{75}Zr_{25}$	2.8	30.0	64.0	3.2
	$Si_{50}Zr_{50}$	4.3	27.7	64.2	3.8
	$Si_{25}Zr_{75}$	7.4	25.1	65.1	2.5
	$Si_{18}Zr_{82}$	30.2	2.1[a]	61.9	5.9
	$Si_{10}Zr_{90}$	26.9	5.7	59.7	7.8
	Si_5Zr_{95}	32.1	0.0	56.6	11.3
	Si_0Zr_{100}	33.9	0.0	55.5	10.6
	$Si_{50}Zr_{50}$ w	4.2	28.4	65.6	1.7

Note. u, uncalcined catalyst; w, rewashed, recalcined catalyst.

[a] Signal from contamination with a grease containing silicon. Si(2*p*) binding energy = 101.9 eV instead of ~103.4 eV for the other samples.

Figure 2 gives the details of the O1*s* line(s) in the region 540–525 eV for catalysts of series B with different ZrO_2 contents. Two separate lines can be observed whose relative intensity depends on the ZrO_2 content of the mixed oxide. The O1*s* binding energy observed for pure SiO_2 is 533.0 ± 0.2 eV. In Si-rich mixed oxides a second line is observed at 530.8 ± 0.5 eV upon deconvolution. In the mixed oxides the size of the first peak decreases and the size of the second increases as the ZrO_2 content increases. Thus, the peak around 533.0 eV is assigned to oxygen near a Si cation, and the peak around 530.8 eV to oxygen near a Zr cation. The single-oxide ZrO_2 has its O1*s* peak at 530.4 ± 0.2 eV. Line widths (FWHM) of the O1*s* lines observed vary between 1.8 and 2.2 eV.

Figure 3 shows the binding energies of both types of O1*s* as a function of the ZrO_2 content in the mixed oxide. The O1*s* binding energy of oxygen near Si is approximately 532.8 ± 0.2 eV at the Si-rich end and 532.4 ± 0.5 eV at the Zr-rich end of the series. The observed binding energies of O1*s* of oxygen near Zr are lower: they are 531.4 ± 0.5 eV at the Si-rich end and 530.4 ± 0.2 eV at the Zr-rich end of the series. It should be noted, however, that the relative error of the binding energy of the O1*s* line of oxygen related to Si at the Zr-rich end of the series and vice versa is large. Nevertheless, it is obvious from Fig. 3 that the difference in O1*s* binding energies observed is clearly larger between the Si-rich and Zr-rich end of the series for the oxygen associated with Zr than for the oxygen associated with Si.

TABLE 3

Binding Energies of XPS Lines of the Various SiO_2–ZrO_2 Catalysts Calcined at 773 K Using XPS

		Binding energy (eV)						
Series	Catalyst	$Zr3d_{5/2}$	$Zr3d_{3/2}$	$Si2p$	$O_{Si}1s$	$O_{Zr}1s$	$F_{Si}1s$	$F_{Zr}1s$
A	$Si_{100}Zr_0$	—	—	103.7	533.0	—	687.6	—
	$Si_{99}Zr_1$	183.7	185.8	103.7	533.0	—	687.5	—
	$Si_{87}Zr_{13}$	183.6	186.0	103.5	532.9	—	687.5	685.1
	$Si_{75}Zr_{25}$	183.5	185.9	103.3	532.6	531.0	687.3	685.2
	$Si_{50}Zr_{50}$	183.3	185.7	103.1	532.6	531.2	687.2	685.2
	$Si_{25}Zr_{75}$	183.2	185.6	103.3	532.8	531.1	687.5	685.2
	Si_0Zr_{100}	182.3	184.7	—	—	530.3	—	685.0
	$Si_{75}Zr_{25}$ u	183.3	185.7	103.0	532.6	531.0	686.6	684.8
B	$Si_{100}Zr_0$	—	—	103.7	533.0	—	687.5	—
	$Si_{95}Zr_5$	183.7	186.0	103.5	532.8	—	687.3	685.0
	$Si_{90}Zr_{10}$	183.5	185.8	103.3	532.7	—	687.3	685.3
	$Si_{75}Zr_{25}$	183.8	186.1	103.5	532.9	531.6	687.4	685.5
	$Si_{50}Zr_{50}$	183.6	185.9	103.3	532.7	531.3	687.3	685.4
	$Si_{25}Zr_{75}$	183.3	185.7	103.1	532.6	531.2	687.3	685.3
	$Si_{18}Zr_{82}$	182.4	184.7	—	532.1	530.2	—	685.0
	$Si_{10}Zr_{90}$	182.5	184.9	103.3	532.4	530.3	687.7	685.1
	Si_5Zr_{95}	182.8	185.1	103.3	532.3	530.6	—	685.4
	Si_0Zr_{100}	182.6	185.0	—	—	530.5	—	685.3
	$Si_{50}Zr_{50}$ w	183.4	185.8	103.3	532.7	531.3	687.3	685.2

Note. The main C(1*s*) line was set at 284.6 eV. u, uncalcined catalyst; w, rewashed, recalcined catalyst.

Figure 4 gives the surface concentration of oxygen assigned to Si (□), Zr (+), and the total amount (◇), as a function of the ZrO_2 content of the mixed oxides. The total concentration is shown to be approximately 66 at% on the condition that the F concentration is low (<2 at%). Although, at high F concentration the O concentration drops, the sum of the surface concentrations of O and F (△) is still around 66 at%. This seems strange at first sight since the valency of oxygen is twice that of fluorine. When F is present preferentially at defects (surface hydroxyls), however, one F atom may substitute for one O atom. Note that the amount of oxygen associated with Zr (+) indeed increases as a function of ZrO_2 content in the mixed oxide, which supports our assignments of the oxygen lines to Zr and Si, respectively. Furthermore, it is clear that the various concentrations do not vary smoothly as a function of Zr content. Below, in a discussion on surface cation concentrations, we will deal with this phenomenon in detail.

Figure 5 gives the XPS spectra of the Zr3*d* lines ($3d_{3/2}$ and $3d_{5/2}$) and Fig. 6 gives the Si2*p* spectra. It can be seen that the

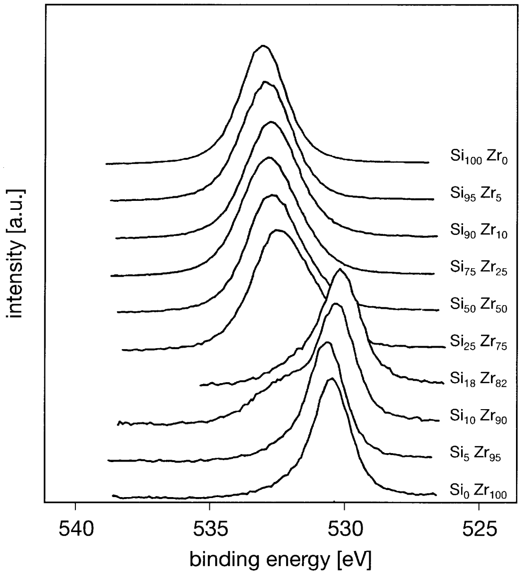

FIG. 2. O1*s* XPS spectra of SiO_2–ZrO_2 mixed and single oxides of series B.

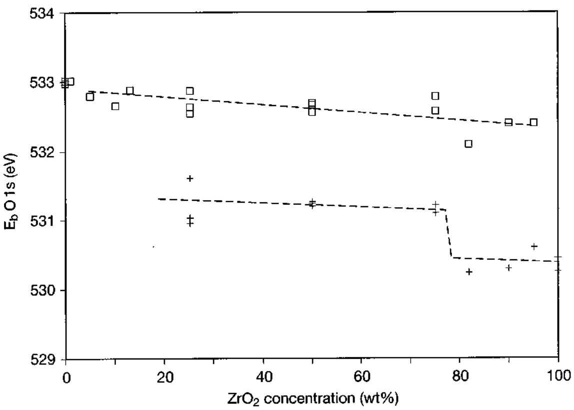

FIG. 3. Binding energy of two O1*s* lines as a function of ZrO_2 content (wt%) in the mixed oxide. □, line assigned to SiO_2; +, line assigned to ZrO_2.

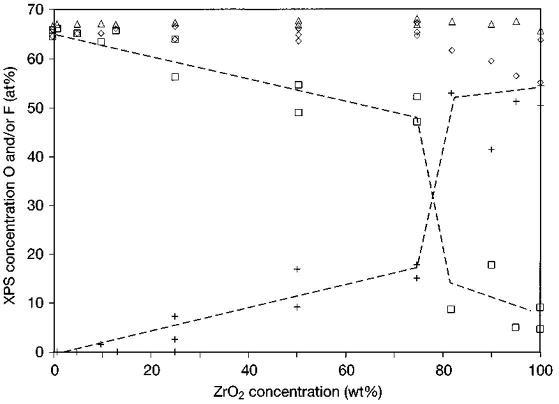

FIG. 4. Surface O concentration (atom %) determined using XPS, as a function of ZrO_2 content (wt%) in the mixed oxide. □, O assigned to Si; +, O assigned to Zr; and ◇, total O concentrations. △, Sum of O and F concentration.

Zr3*d* lines in the mixed oxides shift when the ZrO_2 content increases to 82 wt% or more. The Si2*p* line on the other hand is roughly in the same position for all catalysts studied. Line widths (FWHM) for the $Zr3d_{5/2}$ lines are between 1.6 and 2.0 eV and for the Si2*p* lines they are between 1.7 and 2.3 eV.

The binding energies of the $Zr3d_{5/2}$ electrons and the Si2*p* electrons as a function of the ZrO_2 content in the mixed oxide are given in Figs. 7a and 7b, respectively. The binding energy of $Zr3d_{5/2}$ in the single-oxide ZrO_2, 182.5 ± 0.1 eV, is in agreement with literature values (18, 19). The position of this line for catalysts containing 82 wt% or more ZrO_2 is approximately unaltered. For samples containing 75 wt% ZrO_2 or less, however, the $Zr3d_{5/2}$ binding energy is on an average 1.0 eV higher (ranging from 0.6 to 1.2 eV, absolute error ±0.1 eV) indicating a higher charge on the Zr cation (see further under Discussion). The Si2*p* binding energy is nearly constant, at 103.3 eV (varying between 103.1 and 103.5 eV; absolute error ±0.1 eV) for the mixed oxides. The single-oxide SiO_2 has a Si2*p* line at 103.7 ± 0.1 eV, in agreement with literature values for SiO_2 (18, 19).

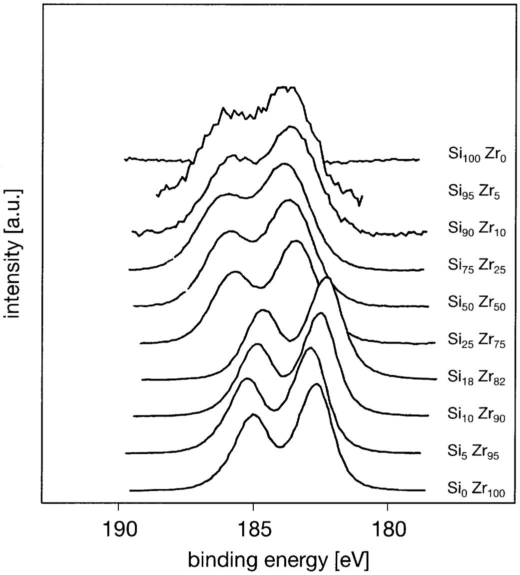

FIG. 5. Zr3*d* XPS spectra of the SiO_2–ZrO_2 mixed and single oxides of series B.

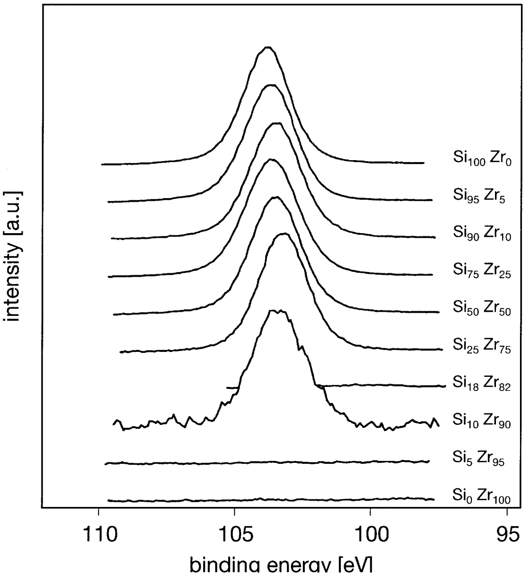

FIG. 6. Si2*p* XPS spectra of the SiO_2–ZrO_2 mixed and single oxides of series B.

In Fig. 8 the surface concentration of Zr, determined from the XPS data, is given as a function of the bulk concentration. The solid line indicates a surface concentration equal to the bulk concentration (i.e., no surface enrichment or depletion). It is clear that the surface Zr concentration is significantly lower than the bulk concentration for catalysts containing 75 wt% ZrO_2 or less. On average the ratio Zr_{XPS}/Zr_{bulk} amounts to 0.50 ± 0.13. Note that the uncalcined $Si_{75}Zr_{25}$ catalyst (indicated by +) is poor in Zr on the surface, too. This excludes effects of the calcination such as phase separation from being responsible, and means that ZrO_2 precipitated faster than SiO_2. Most probably differences in the rate of precipitation cause the surface depletion in Zr (1). Catalysts containing 82 wt% ZrO_2 or more have surface Zr concentrations roughly equal to, or even enriched, compared to bulk concentrations. XRD measurements show that these specimens have the baddeleyite structure. A surface depletion similar to that observed in Zr in our mixed oxides was also reported by Slinkin *et al.* (12). Also the ratio Zr_{XPS}/Zr_{bulk} of approximately 0.6 reported by them compares well with our measurements.

In all spectra F1*s* lines can be observed from fluorine. Detailed XPS spectra of the F1*s* region, 695–680 eV, are given in Fig. 9. As with O1*s*, two F1*s* lines are observed, of which one is ascribed to F near Zr (∼685.2 eV) and the other to F near Si (∼687.4 eV). Series B contains more F (on average) on the catalyst surface than series A. For

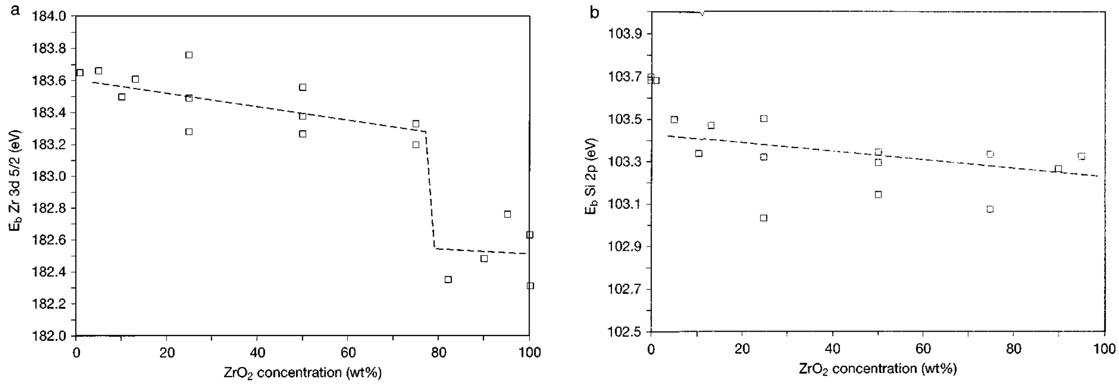

FIG. 7. Binding energy of (a) Zr3$d_{5/2}$ and (b) Si2p as a function of ZrO$_2$ content (wt%) in the mixed oxide.

the Si$_{50}$Zr$_{50}$ sample of series B an acid wash of the catalyst followed by a recalcination at 823 K was performed, resulting in a lower fluorine concentration. The acid wash was performed with diluted HNO$_3$, at the constant pH of 2.0, for 8 h at room temperature followed by a thorough water wash. The surface F concentration dropped from 3.8 to 1.7 at% due to this washing procedure, and all other concentrations were virtually unchanged. Thus we conclude that very small differences in the precipitation procedure may have affected the residual F content in the mixed oxides of the two series and that this fluorine (or at least part of it) resides on the outermost surface layer. Note that also the binding energies of characteristic lines are unchanged after the acid wash (see Table 3). Apparently, fluorine does not affect the chemical state of Si, Zr, and O to a large extent, as was concluded earlier (1).

DISCUSSION

The binding energies observed, especially for the Zr3d electrons and the O1s electrons ascribed to oxygen near Zr^{4+}, are found to be strongly dependent on the composition of the mixed oxide. These shifts may give information on the actual charge on, e.g., the Zr cation in the mixed oxide. In Fig. 10 the O1s binding energy of the oxygen near zirconium is plotted as a function of the Zr3$d_{5/2}$ binding energy. It can be seen that all data fall on a straight line with a slope of 1: the difference in binding energy is roughly constant and amounts to 347.82 ± 0.12 eV. Furthermore, it is clear from the figure that catalysts with $\geq$82 wt% ZrO$_2$ are grouped at one end of the plot (lower binding energies), whereas those with $\leq$75 wt% ZrO$_2$ are grouped at the other end (higher binding energies). Data on catalysts containing less than 25 wt% ZrO$_2$ are omitted from Fig. 10. The intensity of the O1s line is very low compared with the O1s of oxygen near silicon, making it very difficult to determine the exact peak position and causing a large uncertainty in the O1s binding energy.

Figure 11 shows the O1s binding energy of oxygen identified as being near Si^{4+} as a function of the Si2p binding

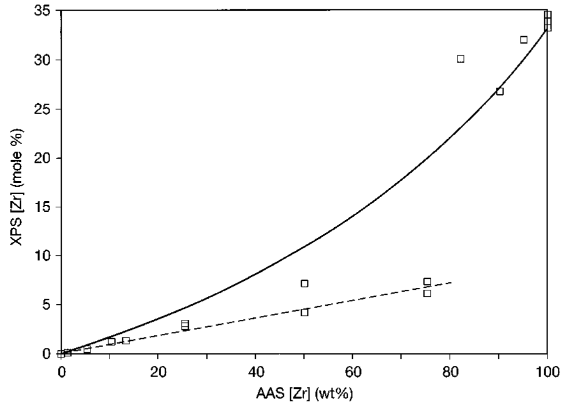

FIG. 8. Surface Zr concentration (at.%) determined using XPS, as a function of the bulk ZrO$_2$ content (wt%) in the mixed oxide.

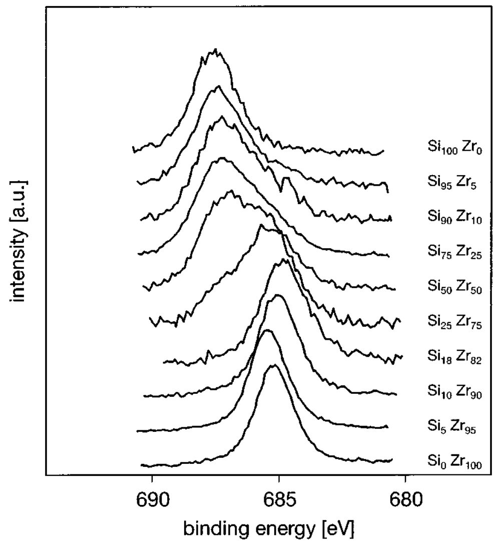

FIG. 9. F1s XPS spectra of the SiO$_2$–ZrO$_2$ mixed and single oxides of series B.

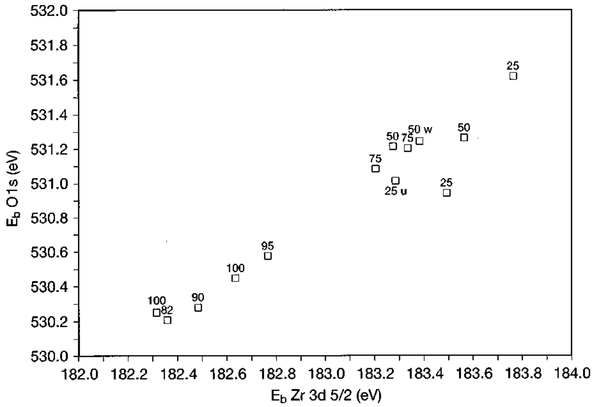

FIG. 10. O1*s* binding energy of the oxygen near Zr as a function of the $Zr3d_{5/2}$ binding energy. The data label gives the ZrO_2 concentration in wt%.

energy. As mentioned earlier the observed shifts in binding energy are smaller than for the Zr-related electrons. Also in this plot all points are situated on a straight line with slope 1. Again, the difference in binding energies is constant, 429.35 ± 0.11 eV. Data on catalysts containing less than 25 wt% SiO_2 are omitted from Fig. 11. Also here the intensity of the O1*s* line of oxygen related to Si is low, again making it difficult to determine the exact peak position and causing a large uncertainty in the binding energy.

The relationship observed for the binding energies of the lines characteristic of the cations on one hand and of the anions (oxygen) on the other hand was reported earlier for SiO_2–Al_2O_3 catalysts (especially zeolites) by Wagner *et al.* (6), Barr and Lishka (7, 8), Okamoto *et al.* (9), and Casamassima *et al.* (10, 11). In Fig. 12, O1*s* binding energies are plotted as a function of Si2*p* binding energies as reported by these authors (6–11) together with our data. All data fall on a single straight line with a slope of one. The difference in binding energy of O1*s* and Si2*p* amounts to 429.30 ± 0.16 eV and is comparable to the difference obtained from our data on its own.

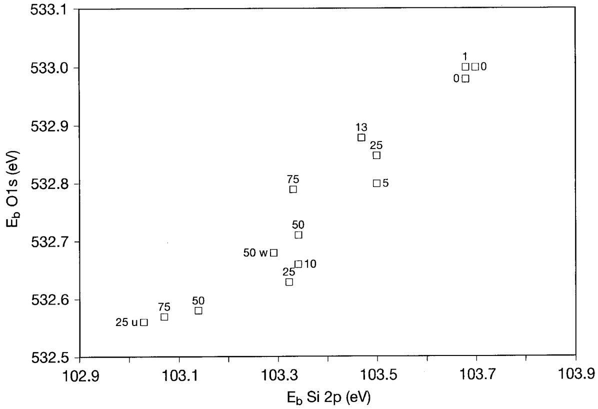

FIG. 11. O1*s* binding energy of the oxygen near Si as a function of the Si2*p* binding energy. The data label gives the ZrO_2 concentration in wt%.

The constancy observed between the binding energies of the relevant electrons, as measured from the characteristic XPS lines, of cations and anions closely associated in an oxide, is striking. Chemical shifts observed for, e.g., the $Zr3d_{5/2}$ and O1s lines in our mixed oxides as a function of ZrO_2 content always occur simultaneously; i.e, the shifts are in the same direction and have roughly the same value. Barr and Lishka (7, 8) also reported this for zeolites. In their opinion, XPS registers "group" rather than "elemental" chemical shifts. Apparently, we observe the same phenomenon for SiO_2–ZrO_2 mixed oxides.

A lowering of the binding energy of Si2*p* in the direction of the binding energy of this line for Si^0 (E_b Si2$p = 99.5$ eV (18, 19)) means a lower positive charge on the Si cation, whereas a lowering of the O1s binding energy implies a higher electron density on O (higher base strength of oxygen). Note that the binding energy of the O1s line of solid O_2 is 538.1 eV, which is derived from a value of 543.1 eV for gas-phase O_2 (22), corrected for the solid–gas work function (23). The simultaneous decrease in the binding energies of O1*s* and Si2*p* indicates a stronger covalency of this Si–O bond in the mixed oxides. As was concluded earlier by Barr and Lishka (7, 8), the increase in covalent character of Si–O bonds in mixed oxides leads to a larger number of Brønsted acid sites. They report that zeolites with a low Si/Al ratio have both a very low O1*s* binding energy (530.4 eV) and a low Si2*p* binding energy (101.1 eV). These catalysts are known to have a high number of Brønsted acid sites. The low O1*s* binding energy is indicative of a high base strength for the oxygen, however, implying a low acid strength of the proton. Moreover, Barr and Lishka report a relationship between the Si/Al ratio of the mixed oxides and the binding energy of both O1*s* and Si2*p* (7): binding energies are lower as the Si/Al ratio drops. Thus, the covalency of the Si–O bond increases as the Si/Al ratio drops, and consequently the number of Brønsted acid sites increases.

In our study we observe only a slight drop in the binding energies of O1*s* and Si2*p* when the ZrO_2 content of the mixed SiO_2–ZrO_2 catalyst increases (see Figs. 3, 7b, and 11). This can be explained with a very small decrease in the positive charge on the Si cation and a higher electron density (base strength) on the oxygen (increase of the covalency of Si–O bonds). This means the generation in parallel of a small number of Brønsted acid sites since protons are needed to balance the excess of negative charge on the oxygen atom. However, no judgment on their strength (H_0) can be given.

The effects measured on the binding energies of $Zr3d_{5/2}$ and O1*s* ascribed to oxygen near zirconium are much larger and opposite to the effects observed with Si–O units. The binding energy of $Zr3d_{5/2}$ in mixed oxides containing ≤75 wt% ZrO_2 is clearly higher than the binding energy

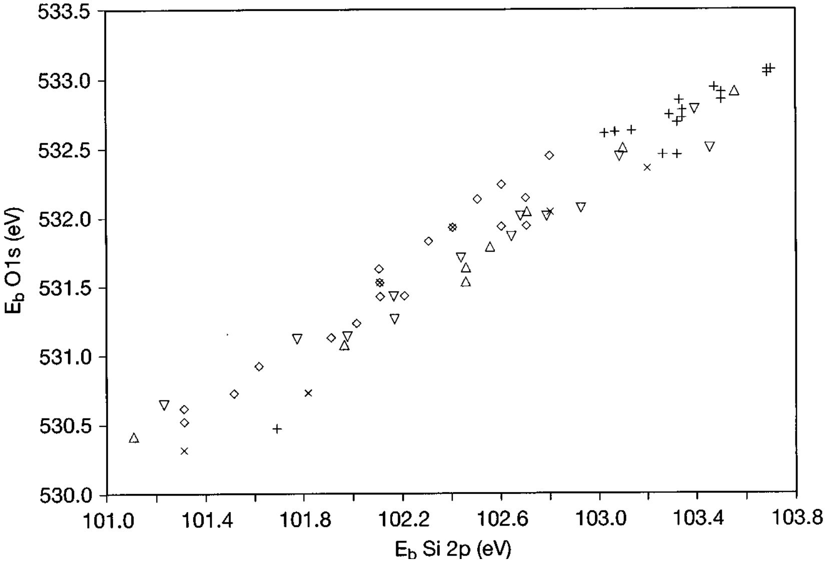

FIG. 12. O1*s* binding energy of the oxygen near Si as a function of the Si2*p* binding energy of various authors compared to our work. ∇, Wagner *et al.* (6); △, Barr and Lishka (7, 8); ◇, Okamoto *et al.* (9); ×, Casamassima *et al.* (10, 11); and +, our work.

in the single oxide ZrO_2 or in mixed oxides containing ≥82 wt% ZrO_2. This implies a higher positive charge on the Zr cation (binding energy of $3d_{5/2}$ electrons for Zr^0 is 178.8 eV (18, 19)). Moreover, the binding energy of O1*s* of oxygen near zirconium is clearly higher in mixed oxides containing ≤75 wt% ZrO_2 than for the single-oxide ZrO_2 and mixed oxides containing ≥82 wt% ZrO_2. This is indicative of a lower electron density on the oxygen atom. This simultaneous increase in the binding energies implies a higher ionicity of the Zr–O bond in the mixed oxides. The higher positive charge on zirconium is indicative of the presence of (strong) Lewis acid sites (electron acceptors). This effect has been found already for SiO_2–ZrO_2 mixed oxides by Slinkin *et al.* (12), in their study on three mixed oxides (3, 10, and 15 wt% ZrO_2). Slinkin *et al.* report only an average binding energy for O1*s* and hence they discuss only the overall ionicity of the mixed oxide. They state, however, that the ionicity of the mixed oxide increases compared with the single oxides. In our opinion this is also indicative of the occurrence of (enhanced) Lewis acidity.

We state that XPS shows that mixed SiO_2–ZrO_2 oxides (with ZrO_2 contents of 75 wt% and less) contain strong Lewis acid sites and may contain also a few additional Brønsted acid sites of unknown acid strength. In our opinion, the Lewis acidity is related to the Zr cation ($Zr^{\delta+}$, electron-deficient sites), whereas the Brønsted acid sites are related to slightly more covalent Si–O bonds (due to the presence of Zr in their neighborhood), e.g., Si–OH–Zr. The increased positive charge on the Zr cation seems to be the dominant feature, determining the overall acidity of our SiO_2–ZrO_2 mixed oxides. These findings are in agreement with our DRIFTS study (2) on ammonia-treated SiO_2–ZrO_2 mixed oxides which gives evidence for the presence of strong Lewis acid sites besides weaker Brønsted acid sites.

In the literature several models have been presented for the prediction of the acidity in mixed oxides from single oxide properties. Tanabe *et al.* (24, 25) postulated a model based on local changes in an oxide matrix which occur upon introduction of a second oxide. They argued that the cations of the dopant oxide maintain their original coordination number, even when mixed, but that the anions (oxygen) adopt the coordination number of the host-oxide oxygens. This can lead to a charge imbalance, which introduces Lewis acidity when an excess of positive charge occurs and Brønsted acidity when an excess of negative charge occurs (increased covalency; protons compensate this imbalance). For a SiO_2–ZrO_2 mixed oxide, Brønsted acidity is predicted at the SiO_2-rich end of the series, and Lewis acidity at the ZrO_2-rich end.

The model of Kung (26) states that acidity may be generated when differences in electrostatic potential occur for a cation A (oxide stoichiometry AO_y) in a matrix BO_z. It also takes into account the changes which must occur in the matrix to balance the stoichiometry difference between the two oxides. For oxides having the same stoichiometry, as is the case for SiO_2 and ZrO_2, the resulting acidity in the chemically mixed oxides depends solely on the difference in ionicity or covalency of the single oxides.[2] Of these, ZrO_2

---

[2] In our opinion Kung makes an error in Table III of his publication. In this table he summarizes his model and states that Lewis sites are to be expected at the substituting cation site when the matrix oxide is more ionic. On the other hand he states that a lower lattice self-potential of the matrix oxide leads to an electrostatically more stable guest cation, and thus Lewis acid sites. A lower lattice self-potential, however, means a more covalent oxide.

is the most ionic, as follows from the ion electronegativity. The electronegativity $\chi = 12.1$ for Si^{4+}, and $\chi = 10.1$ for Zr^{4+}, as calculated from Pauling electronegativities for the elements (27) and the model of Misono *et al.* (28) for the electronegativity of ions. The lattice self-potentials (−48.5 V on average for SiO_2 vs −42.3 V for ZrO_2 (24)) also indicate that ZrO_2 is more ionic. This means that Lewis acidity is predicted when a Zr cation is incorporated in a more covalent SiO_2 matrix, at the site of the substituting ion.

The Kung model seems to be more appropriate in our situation. For our SiO_2–ZrO_2 mixed oxides Lewis acid sites are present, most probably at the Zr site, as follows from the shifts in binding energies of relevant XPS lines. These are explained with higher ionicity for Zr–O bonds, which is in line with Kung's assumption on electrostatic stability of guest cations in oxides.

CONCLUSIONS

The XPS study of SiO_2–ZrO_2 mixed oxides described in this paper yields valuable insight into the surface structure of the catalysts, and in the acidity generated upon the chemical mixing of the two components. The binding energies of the various electrons, associated with Si, Zr, and O present in the mixed oxides, compared with those in the single oxides, yield information on both the actual charge associated with the atom and on the ionicity or covalency of the metal–oxygen bonds. This information is indicative of the acid properties of the oxides. An increased charge on cations is associated with Lewis acidity, whereas an increased electron density on oxygen leads to a higher number of Brønsted acid sites. Thus, in the mixed SiO_2–ZrO_2 oxides (containing ≤ 75 wt% ZrO_2) an increased number of Lewis acid sites is found, in our opinion associated with the Zr cation. Besides this, a small increase is measured in the number of Brønsted acid sites, which probably consist of silanols in the vicinity of zirconium. The Kung model is more appropriate than that of Tanabe *et al.* in describing the acidity in our SiO_2–ZrO_2 mixed oxides.

Catalysts containing ≤ 75 wt% ZrO_2 show a surface depleted in Zr pointing to a faster precipitation rate of ZrO_2 compared to SiO_2. Catalysts containing ≥ 82 wt% ZrO_2 show surface Zr concentrations roughly in agreement with bulk concentrations.

ACKNOWLEDGMENTS

The samples were prepared by Mr J. van der Spoel and Dr. E. C. Kruissink. Mr. J. Blok and Mr. P. van Oeffelt performed the measurements of the BET specific surface area. XRD measurements were performed by Mr. Ramaekers and Dr. J. Moonen. The authors are indebted to Dr. R. van Hardeveld for valuable remarks and a critical review of the manuscript. DSM Research is acknowledged for their permission to publish this work.

REFERENCES

1. Bosman, H. J. M., Kruissink, E. C., van der Spoel, J., and van den Brink, F., *J. Catal.* **148**, 660 (1994).
2. Bosman, H. J. M., van Heel, J. P. C., and Lefferts, L., submitted for publication.
3. Makarov, A. D., Boreskov, G. K., and Dzisko, V. A., *Kinet. Katal.* **2**, 84 (1961).
4. D'yakonov, S. S., Lygin, V. I., Shalumov, B. Z., Shepalin, K. L., Kuznetsov, A. I., Kostina, V. M., and Rastorguev, Y. I., *Izv. Akad. Nauk. SSSR. Neorg. Mater.* **20**, 97 (1984).
5. Thielsch, R., Meiling, W., and Goering, E., *Vacuum* **41**, 1147 (1990).
6. Wagner, C. D., Passoja, D. E., Hillery, H. F., Kinisky, T. G., Six, H. A., Jansen, W. T., and Taylor, J. A., *J. Vac. Sci. Technol.* **21**, 933 (1982).
7. Barr, T. L., and Lishka, M. A., *J. Am. Chem. Soc.* **108**, 3178 (1986).
8. Barr, T. L., *Zeolites* **10**, 760 (1990).
9. Okamoto, Y., Ogawa, M., Maezawa, A., and Imanaka, T., *J. Catal.* **112**, 427 (1988).
10. Casamassima, M., Darque-Ceretti, E., Etcheberry, A., and Aucouturier, M., *Appl. Surf. Sci.* **52**, 205 (1991).
11. Casamassima, M., Darque-Ceretti, E., Etcheberry, A., and Aucouturier, M., *J. Mater. Sci.* **28**, 3997 (1993).
12. Slinkin, A. A., Klyachko, A. L., Shpiro, E. S., Kapustin, G. I., Kucherova, T. N., Stakheev, A. Yu., and Ermolov, L. V., *Kinet. Katal.* **32**, 725 (1991).
13. Seah, M. P., *Surf. Interface Anal.* **14**, 488 (1989).
14. Berresheim, K., Mattern-Klosson, M., and Wilmers, M., *Fresenius' J. Anal. Chem.* **341**, 121 (1992).
15. Nöller, H. G., Polaschegg, H. D., and Schillalies, H., *J. Electron Spectrosc. Relat. Phenom.* **5**, 705 (1974).
16. Scofield, J. H., *J. Electron Spectrosc. Rel. Phenom.* **8**, 129 (1976).
17. Briggs, D., and Seah, M. P. (Eds.), "Practical Surface Analysis: Auger and X-Ray Photoelectron Spectroscopy," 2nd ed., Vol. 1, Appendix 2. Wiley, Chichester, 1990.
18. Mullins, W. M., and Averbach, B. L., *Surf. Sci.* **206**, 29 (1988).
19. Stephenson, D. A., and Binkowski, N. J., *J. Non-Cryst. Solids* **22**, 399 (1976).
20. Briggs, D., and Seah, M. P. (Eds.), "Practical Surface Analysis: Auger and X-Ray Photoelectron Spectroscopy," 2nd ed., Vol. 1, Chapter 5. Wiley, Chichester, 1990.
21. Moulder, J. F., Stickle, W. F., Sobol, P. E., and Bomben, K. D., "Handbook of X-Ray Photoelectron Spectroscopy." Perkin–Elmer, Eden Prairie, MN, 1992.
22. Siegbahn, K., Nordling, C., Johansson, G., Hedman, J., Hedén, P. F., Hamrin, K., Gelins, U., Bergmark, T., Werme, L. O., Manne, R., and Baer, Y., "ESCA Applied to Free Molecules." North-Holland, Amsterdam, 1969.
23. Wagner *et al.* (Ref. (6)) give a value of 5.0 eV for gaseous Si-containing components, and Brundle, C. R., *in* "Electronic Structure and Reactivity of Metal Surfaces" (E. G. Derouane and A. A. Lucas, Eds.). Plenum, New York, 1976, gives a value of 5.2 eV for N_2O as a correction for the gas–solid work function.
24. Tanabe, K., Misono, M., Ono, Y., and Hattori, H., *Stud. Surf. Sci. Catal.* **51**, 1 (1989).
25. Tanabe, K., Sumiyoshi, T., Shibita, K., Kiyoura, T., and Kitagawa, J., *Bull. Chem. Soc. Jpn.* **47**, 1064 (1974).
26. Kung, H. H., *J. Solid State Chem.* **52**, 191 (1984).
27. Pauling, L., "The Nature of the Chemical Bond." Cornell Univ. Press, Ithaca, NY, 1960.
28. Misono, M., Ochiai, E., Saito, Y., and Yoneda, Y., *J. Inorg. Nucl. Chem.* **29**, 2685 (1967).